ELSEVIER

Contents lists available at ScienceDirect

#### Cells & Development

journal homepage: www.journals.elsevier.com/cells-and-development





# Developmental programming by maternal obesity alters offspring lifespan and immune responses in a diet- and sex-specific manner<sup>☆</sup>

Seyhmus Bayar <sup>a</sup>, Lea Seep <sup>b</sup>, Karolína Doubková <sup>c,d</sup>, Jelena Zurkovic <sup>e</sup>, Margret H. Bülow <sup>f</sup>, Katrin Kierdorf <sup>g,h</sup>, Reinhard Bauer <sup>i</sup>, Christoph Thiele <sup>e</sup>, Gaia Tavosanis <sup>c,d</sup>, Jan Hasenauer <sup>b</sup>, Elvira Mass <sup>a,\*</sup>

- <sup>a</sup> Developmental Biology of the Immune System, Life & Medical Sciences (LIMES) Institute, University of Bonn, 53115 Bonn, Germany
- b Computational Life Sciences, Life & Medical Sciences (LIMES) Institute and Bonn Center for Mathematical Life Sciences, University of Bonn, 53115 Bonn, Germany
- <sup>c</sup> German Center for Neurodegenerative Diseases (DZNE), Dynamics of Neuronal Circuits Group, 53127 Bonn, Germany
- <sup>d</sup> Institute for Developmental Biology, RWTH Aachen University, Aachen 52074, Germany
- <sup>e</sup> Biochemistry & Cell Biology of Lipids, Life & Medical Sciences (LIMES) Institute, University of Bonn, 53115 Bonn, Germany
- f Neuronal Cell Metabolism, Life & Medical Sciences (LIMES) Institute, University of Bonn, 53115 Bonn, Germany
- g Institute for Infection Prevention and Control, Faculty of Medicine, University of Freiburg, 79106 Freiburg, Germany
- <sup>h</sup> CIBSS-Center for Integrative Biological Signaling Studies, University of Freiburg, 79104 Freiburg, Germany
- i Department of Molecular Developmental Biology, Life & Medical Sciences (LIMES) Institute, University of Bonn, 53115 Bonn, Germany

#### ARTICLE INFO

# Keywords: Maternal obesity Drosophila melanogaster Developmental reprogramming Metabolism Lifespan Neurodegeneration Macrophages Hemocytes Plasmatocytes

#### ABSTRACT

Maternal obesity is a growing health concern that predisposes offspring to metabolic dysfunction, immune system alterations, and neurodegenerative disorders. To investigate the intergenerational effects of maternal obesity, we used *Drosophila melanogaster* exposed to high-sugar (HSD) and high-fat diets (HFD) before mating. We found that maternal diet-induced obesity significantly altered offspring lifespan, immune responses, and neuronal health in a sex- and diet-specific manner. Male offspring were particularly susceptible, exhibiting reduced lifespan, impaired climbing ability, and increased axonal degeneration, especially following maternal HFD exposure. Transcriptomic analyses revealed age-dependent and diet-specific changes, with males showing pronounced alterations at 50 days of age. Developmental programming of hemocytes (blood-like cells) played a crucial role in these outcomes, as knockdown of key immune pathways such as *Relish* and *upd3* in hemocytes further influenced lifespan in a diet-specific manner. These findings highlight the complex interplay between maternal diet and immune function, underscoring the impact of maternal obesity-induced imprinting on immune cells and subsequent long-term health consequences. Our study provides new insights into conserved mechanisms linking maternal metabolic health to offspring outcomes and emphasizes the continued need for animal models to understand intergenerational health impacts.

#### 1. Introduction

The global prevalence of obesity has reached endemic levels, with maternal obesity emerging as a significant and rapidly growing health concern (Timpson et al., 2024; Catalano and Ehrenberg, 2006). Obesity during pregnancy heightens the risk of gestational diabetes, miscarriage, and preeclampsia, while predisposing offspring to developmental abnormalities and long-term metabolic issues such as type 2 diabetes and cardiovascular disease (Sureshchandra et al., 2023; Brookheart and Duncan, 2016). Studies in both humans and rodents have identified

associations between maternal overnutrition and factors like metabolic disorders, epigenetic changes, mitochondrial dysfunction, insulin resistance, endoplasmic reticulum stress, and immune system disruption (Catalano and Ehrenberg, 2006; Brookheart and Duncan, 2016; Koemel et al., 2022; Phang et al., 2020; Napso et al., 2022). Both human and animal studies suggest these impacts can persist through the lifespan of offspring, leading to a higher risk of chronic disorders in adulthood (Denizli et al., 2022a). However, the precise molecular mechanisms linking these factors to maternal obesity remain unclear.

Although the effects of maternal obesity on offspring's metabolic

E-mail address: elvira.mass@uni-bonn.de (E. Mass).

https://doi.org/10.1016/j.cdev.2025.204040

Received 10 January 2025; Received in revised form 30 May 2025; Accepted 4 July 2025 Available online 11 July 2025

2667-2901/© 2025 The Authors. Published by Elsevier B.V. This is an open access article under the CC BY-NC license (http://creativecommons.org/licenses/by-nc/4.0/).

 $<sup>^{\</sup>star}$  This article is part of a Special issue entitled: 'Tissue Biology' published in Cells & Development.

<sup>\*</sup> Corresponding author.

health are well-documented, its impact on ageing and longevity remains poorly understood. Emerging studies indicate that maternal obesity may promote premature ageing in offspring by increasing oxidative stress, causing metabolic dysfunction, and altering age-associated gene expression, particularly in the liver, in a sex-dependent manner (Lomas-Soria et al., 2023; Rodríguez-González et al., 2019). Furthermore, maternal obesity has been shown to shorten telomere length, a key biomarker of ageing, in oocytes and early embryos in mice (Ge et al., 2021). In humans, maternal pre-pregnancy BMI negatively correlates with telomere length in cord blood and placenta (Martens et al., 2016). These findings suggest that maternal obesity may influence not only the metabolic health but also the ageing process and longevity of the next generation.

Maternal obesity is also associated with significant changes in immune system development and function. Long-lived cells, such as tissueresident macrophages, are key mediators of intergenerational information transfer from mother to offspring (Viola et al., 2024; Mass and Gentek, 2021). For instance, maternal obesity disrupts neurodevelopment by altering microglial function in a sex- and region-specific manner. These changes, mediated in part by toll-like receptor 4 signaling and increased endotoxin levels, lead to neuroinflammation, impaired serotonin availability, and an increased risk of neuropsychiatric disorders, particularly in male offspring (Viola et al., 2024; Ceasrine et al., 2022). Additionally, Kupffer cells, the liver-resident macrophages, in offspring from obese mothers exhibit persistent molecular changes, which cause increased lipid accumulation in hepatocytes and fatty liver disease (Huang et al., 2025). These macrophage alterations can last into adulthood, suggesting that maternal obesity has long-term impacts on immune cell function and overall tissue health. Understanding how maternal obesity shapes tissue and cell functions in offspring is crucial for developing strategies to prevent and mitigate these adverse outcomes.

In this study, we used Drosophila melanogaster as a model organism to investigate the effects of maternal obesity on the next generation. One reason for using Drosophila is that macrophages, known as plasmatocytes in this species, represent >95 % of all hemocytes. Additionally, many pathways and molecular responses of macrophages to dietary challenges are conserved between mammals and invertebrates (Cox et al., 2021; Woodcock et al., 2015; Mase et al., 2021). Using two maternal obesity models induced by high-sugar (HSD) or high-fat diets (HFD), we identified pathways involved in neurodegeneration and immune responses that are persistently altered in the offspring. Notably, these changes were sex- and diet-specific, with males being more prone to axonal degeneration, decreased life span, and reduced overall fitness. Further, our findings demonstrate that the developmental programming of hemocytes by maternal obesity influences Drosophila lifespan in a diet- and immune-pathway-specific manner, highlighting the interplay between maternal diet, immune function, and lifespan.

#### 2. Material and methods

#### 2.1. Fly strains and husbandry

All flies were maintained on control diet (CD) and raised in light/dark cycles (12:12 h) in a climate-controlled incubator at 25 °C with constant humidity. As wildtype line w<sup>1118</sup> flies (Bloomington, #6326) were used. To generate hemocyte-specific knockdown, CD males of y[1] sc[\*] v[1] sev[21]; P{y[+t7.7] v[+t1.8] = TRiP.HMS00070}attP2 (UAS-Rel-RNAi) (Bloomington, #33661), or (y[1] sc[\*] v[1] sev[21]; P{y[+t7.7] v[+t1.8] = TRiP.HMS00646}attP2) (UAS-Upd3-RNAi) (Bloomington, #32859) transgenic lines, were bred with w<sup>1118</sup>;HmlΔ-Gal4, UAS-2xeGFP (Hml-Gal4 > UAS-2xeGFP) (Bloomington, #30140) transgenic driver line, exposed to CD, HSD or HFD premating. For axonal degeneration experiments, the GMRwhiteRNAi;GMR-Gal4/Cyo;UAS-tubulinGFP/MKRS line, generated using the GMRwhite-RNAi transgenic line (Bloomington, #32067) in combination with UAS-tubulinGFP

(Bloomington, #7374) and *GMR-Gal4* (Bloomington, #1104) (Richard et al., 2022a), was exposed to CD, HSD or HFD and subsequently bred with  $w^{1118}$  CD males. A commercially obtainable food substrate, Nutrifly (Genesee Scientific, 66–112) containing essential nutrients was used to house all lines. The CD was prepared by mixing 176 g of Nutri-fly with 10 ml 10 % nipagin (Sigma-Aldrich, 99-76-3) in ethanol and 4,8 ml propionic acid (Sigma-Aldrich, 79-09-4) per liter of food solution. 20 % coconut oil (BioBio) or sucrose (Sigma-Aldrich, S1888) were added to the CD to prepare HFD and HSD, respectively. For all experiments 10–15 virgin females were mated with 10 males.

#### 2.2. Measurement of body weight

Single flies were anaesthetized with  ${\rm CO_2}$  and transferred to a sterile petri dish over ice, and their body weight was rapidly measured using a precision scale.

#### 2.3. Glucose level measurement

The assay reagent was prepared by mixing 39.2 ml of the glucose oxidase/peroxidase reagent (GO) (Sigma-Aldrich, G3660) with 0.8 ml of the o-dianisidine reagent (Sigma-Aldrich, D2679). All experimental steps were carried out on ice to prevent the enzymatic digestion of glycogen and trehalose. For measuring glucose, all flies were starved for 1 h. Two flies were pooled per sample and homogenized in 100 μl of PBS. Subsequently, the homogenate was spun at 2000 g for 5 min, and the supernatant was heated at 70 °C for 10 min. By diluting the glucose standard solution (Sigma-Aldrich, G3285), glucose standards of 0, 0.02, 0.04, 0.08, and 0.16 mg/ml were prepared for the standard curve. Using a clear-bottomed 96-well plate, 50 µl of each standard sample was placed into a well and mixed with 50  $\mu l$  of the assay reagent. The samples were incubated for 45 min at 37 °C to ensure the reactions were completed. To stop the reaction,  $100 \mu l$  of 1.8 M sulfuric acid was added to each well. The absorbances were measured utilizing a plate reader at 540 nm.

#### 2.4. Lipidomics

For isolation of lipid species 500 µl of extraction mix ((CHCl<sub>3</sub>/MeOH 1/5 comprising internal standards: 250 pmol PE (31:1), 84 pmol PI (34:0), 472 pmol PC (31:1), 28 pmol CL (56:0), 98 pmol PS (31:1), 56 pmol PA(31:1), 51 pmol PG (28:0), 39 pmol LPA (17:0), 55 pmol GlcCer (12:0), 45 pmol Car (15:0), 38 pmol LPE (17:0), 32 pmol Cer (17:0), 240 pmol SM (17:0), 340 pmol TG (50:1-d4), 64 pmol DG (31:1), 111 pmol CE (17:1), 103 pmol MG(17:1),35 pmol LPC (17:1), 724 pmol Chol (d6)), were homogenized with samples (one fly per condition and sample), followed by resuspension in another 300 µl of the extraction mix. The homogenate was then sonicated for 30 min using a bath sonicator to break cellular material and allow effective extraction. After the sonication, samples were centrifuged at 20,000g for 2 min, facilitating the removal of cellular debris. Subsequently, the supernatant was pipetted into a new Eppendorf tube. 200 μL chloroform (Merck Millipore, 1024421000) and 800  $\mu L$  of 1 % acetic acid solution in water were homogenized to purify the sample further. The homogenate was then stirred manually for 5 s and centrifuged at 20,000g for 2 min for phase separation. The phase of lipids was then transferred into the fresh Eppendorf tube and evaporated in speed vac for 15 min at 45 °C, resuspended with 100 µl of spray buffer (8/5/1 isopropanol/methanol/ H<sub>2</sub>O (all LC-MS grade) containing 10 mM ammonium acetate), and sonicated for 5 min to ensure homogenous distributions of the analytes. Samples were measured via a Thermo Q Exactive Plus spectrometer with a HESI II ion source in the  $\mu l/\text{min}$  rate for shotgun lipidomics. MS spectra with a resolution of 280,000 were captured in  $100 \, m/z$  windows ranging from 250 to 1200 m/z, followed by acquisition of MS spectra at a resolution of 70,000 in 1 m/z windows from 250 to 1200 in positive mode. Raw files were transformed into mzML files and then loaded into

LipidXplorer software using custom mzML files, which were used to analyze and identify internal standards and samples. The internal standard was utilized to compute absolute amounts to process the data. For each lipid class, raw data were transformed into picomol (pmol), and the mean value of all peaks was acquired based on pmol values. The extracted lipids were quantified and normalized by the body weights of analyzed *Drosophila*.

#### 2.5. Climbing assay

For the climbing assay, 20–25 age-matched flies per group were sorted into new cages (Dominique Dutscher, 789009) once they had hatched. All progeny from CD, HFD, and HSD were then raised on a CD during the experimental step. The flies were recounted and moved into fresh cages a day before the experiments. In the day of the experiment flies were transferred into empty climbing tubes. The climbing ability of the flies was recorded with a smartphone on the day of the investigation. The pictures were imported and scaled using Fiji software. Climbing length was recorded for each fly using the shortcut command "strg+M", which was used to measure the height of the flies from the bottom of the climbing tube. Flies that were not seen at the bottom of the climbing tubes due to the wooden material in which the climbing tubes are placed were documented to have a height of zero.

#### 2.6. Longevity assay

To investigate the longevity, 10–16 flies were allocated per vial containing CD. All experiments had a minimum of three replicates for each condition. The progeny was raised at 25  $^{\circ}$ C, and the number of dead flies was recorded every 3–4 days. Vials were stored vertically and flies stuck to the food on the day of evaluation were excluded from the data curve and statistics. Surviving flies were transferred into fresh vials.

#### 2.7. Bulk-RNA sequencing

#### 2.7.1. Purification of RNA

The samples were stored at -80 °C in 500  $\mu$ l of Qiazol (Qiagen, 79306) until RNA isolation. Five flies were pooled per sample and dietary condition. All samples were randomized and processed in balanced batches across conditions. On the day of the experiment, the workbench and equipment were cleaned with RNase AWAYTM Surface Decontaminant (Fisher Scientific, 11580095). RNeasy UCP Micro Kit (50) (Qiagen, 73934) kit was used for the isolation. The samples were thawed and homogenized using the Precellys®24 (Peqlab) system at 5000 rpm for 15 s, then centrifuged at 13,000g for 30 s, and the supernatant was pipetted to a new tube to remove residual glass beads. The homogenized samples were mixed with chloroform (Merck Millipore, 1024421000) at a 1:5 ratio for RNA extraction and spun for 15 min at 13,000 g at 4 °C. The upper aqueous phase was pipetted to a fresh tube, and 300 µl of absolute ethanol was added. The RNA-containing solution was pipetted into a 2 ml RNeasy MinElute spin column (Qiagen RNeasy MinElute Cleanup Kit) and centrifuged at 8000g for 15 s. All remaining isolation steps were performed as per the manufacturer's instructions. RNA samples were stored at  $-80~^{\circ}$ C until library preparation.

#### 2.7.2. Preparation of libraries and sequencing

For quality control, the Agilent RNA 6000 pico Kit (Agilent Technologies, #5067-1513) and the Agilent 2100 Bioanalyzer were used; the RNA integrity number (RIN) was computed following the manufacturer's instructions to evaluate the RNA's quality and gauge the extent of degradation. All samples had a RIN > 8 and were used for library preparation. Sequencing libraries were prepared using 300 ng of total RNA and the NEBNext RNA Ultra II kit combined with the poly(A) mRNA Magnetic Isolation Module (New England Biolabs). Library preparation was automated on the Beckman i7 liquid handling robot, with parameters set to 9 min of RNA fragmentation and 13 cycles of PCR

amplification. All libraries were pooled and sequenced on the Illumina NextSeq 2000 platform using the P3-50 sequencing kit.

#### 2.7.3. Quantification and analysis

All raw files are publicly available and deposited on GEO (Project ID GSE284632). The obtained reads were aligned and quantified using kallisto (Bray et al., 2016). The organism's transcriptome FASTA files (Genome assembly BDGP6.46) were first used to build an index, followed by quantification from fastq files. The resulting abundance.h5 files were read into R (v. 4.2.0) and merged with annotations from the corresponding genome assembly GTF file to add gene symbols and biotypes, while unnamed transcripts were excluded. The tximport (v. 1.24.0) (Soneson et al., 2015) and DESeq2 (v. 1.36.0) (Love et al., 2014) packages were used to generate a summarizedExperiment (Morgan et al., 2020) object. A final gene collection of 12,631 was kept after preprocessing, which included retaining only protein-coding genes and removing genes with fewer than ten counts in >25 % of the data.

Principal component analysis (PCA) was performed using variancestabilized counts. Due to clustering with the opposite sex, which we assume were due to processing errors in the sequencing core facility, the male sample, M8 and female sample, F12, were removed from the data. Subsequently, the dataset was divided into sex-specific subsets, and the smaller sets were subjected to the previously mentioned data processing techniques. The respective gene counts for the male and female sets were 12,614 and 10,481. To eliminate the age-related signature within the sex-specific subsets for PCA analysis, limma's removeBatchEffect function (Ritchie et al., 2015) was applied to the variance-stabilized transformed data. Specifically it fits a linear model whereby age and the interaction between age and sex were used as covariates, while diet served as the primary design factor. The estimated component due to the covariates is subsequently removed from the data. Age and the interaction between age and sex were used as covariates, while diet served as the primary design factor. DESeq2 was used for differential expression analysis with a design that accounted for the two main factors - diet and day - as well as their interaction effect. Respective contrasts were defined in the results function of DESeq2. P. adj < 0.1 was considered significant for a gene, whereas LFC > 0 denoted upregulation and LFC < 0 denoted downregulation. The obtained differentially expressed (DE) sets were compared to identify unique sets specific to each condition. These unique sets were subjected to enrichment analysis using cluster-Profiler (Wu et al., 2021; Yu et al., 2012) and the org.DM.eg.db database resource. The shown enrichment terms are a curated set from all obtained enriched terms. The code to reproduce the depicted results can be obtained from https://github.com/LeaSeep/fly\_sugar, a snapshot is saved to Zenodo and accessible via doi:https://doi.org/10.5281/zenodo .14523856.

#### 2.8. Axonal-degeneration assay

Each maternal group's female and male offspring were placed into new CD cages, with up to 10 flies per cage, and raised for 10 days at 25 °C and 60 % humidity. Control flies experienced a light-dark (LD) cycle in the experiment, while the continuous light group was kept under constant light (LL) for 7 days. The 6 W warm white LED light source (Heitronic) with an illumination level of 10,000 lx was utilized for light exposure, and the light intensity was measured using a Volt Craft MS-1300 photometer (Conrad). LL and LD flies were immobilized on ice for brain dissections, and brains were washed at room temperature  $1 \times$  PBS and fixed with 4 % cold formaldehyde for 50 min. The brains were washed with PBS, including 0.3 % Triton X-100. Next, samples were stained with a primary antibody against mouse anti-Chaoptin (DSHB, 24b10) at a 1:25 dilution and incubated overnight in PBS containing 0.1 % Triton X-100 and 1 % BSA at 4  $^{\circ}$ C. The following day, samples were stained with an anti-mouse Alexa Fluor 594 (Life Technologies) secondary antibody in 1:400 dilution for 2-3 h at room temperature. Ultimately, samples were mounted in their posterior

orientation in Vectashield (Vector Laboratories), to keep their original volume and shape 0.1 mm insect pins were used.

Axonal R7 termini in the z-stack of the whole medulla were imaged with a Zeiss LSM 780 confocal microscope, using a 40× oil immersion objective. The 16-bit images were taken in 1  $\mu m$  fixed z-step, 1024  $\times$  1024 frame size and 1 AU. Images were then analyzed using Fiji software, and semi-automated quantification of R7 termini was performed using Imaris software (Bitplane, 9.7.2. software). Subsequently, a compact 3D mask of R7 termini was generated by automated software developed by Nitta et al., 2023 and R7 axonal terminals were counted (Richard et al., 2022b; Nitta et al., 2023).

#### 2.9. Quantification of hemocytes

 $\mathit{Hml\text{-}GAL4} > \mathit{UAS\text{-}2eGFP}$  flies were immobilized on ice and placed onto slides using a laterally fixed adhesive glue (Pritt, all-purpose glue). Zeiss LSM 880 confocal microscopy was utilized for imaging, with fluorescence excitation set at 488 nm with a  $10\times$  objective. Images were taken with z-stacks of the whole body, with a  $4\times3$  tile scan, a gain of 757, 1 AU pinhole and maximum z-stack, respectively. Image stacks were transformed into 3D with maximum-intensity projections and converted to TIFF format; subsequently, hemocytes were quantified with a 3D object counter at the threshold of 220–240 in Fiji software.

#### 2.10. Statistical analysis

Statistical difference between groups was examined using GraphPad Prism 10. Comparisons for most experiments were tested by one-way ANOVA. The survival assays were analyzed using the Gehan-Breslow Wilcoxon test. Levels of statistical significance are indicated as \* for p < 0.05, \*\* for p < 0.01, \*\*\* for p < 0.001, and \*\*\*\* for p < 0.0001.

#### 3. Results

#### 3.1. Establishment of maternal obesity models

To model maternal obesity in *Drosophila melanogaster*, virgin females were placed on either a high-fat diet (HFD) or a high-sugar diet (HSD) for seven days, with a control diet (CD) group used as a baseline for comparison. These diets were specifically designed to induce obesity-like metabolic states, mimicking maternal obesity to assess its effects on the offspring. The HFD, enriched with 20 % coconut oil, reflects diets high in fat, while the HSD incorporated increased levels of 20 % sucrose, which is commonly used as a diet-induced obesity model in *Drosophila* (Gáliková and Klepsatel, 2018; Heinrichsen et al., 2014; Lee et al., 2020; Musselman et al., 2011; Yang et al., 2023; Huang et al., 2020; Eickelberg et al., 2022).

After seven days of feeding, females from each group were mated with CD-fed males, and their progeny were raised on CD to isolate the impact of maternal nutrition (Fig. 1A). To confirm the establishment of maternal obesity, we first analyzed the body weight of females after exposure to the different diets. Females fed the HFD or HSD showed significant weight loss compared to females on the CD (Fig. 1B), which is consistent with diet-induced obesity models in Drosophila (Musselman et al., 2011; Eickelberg et al., 2022; Nayak and Mishra, 2021; Camilleri-Carter et al., 2019; Musselman et al., 2013; Lourido et al., 2021; Skorupa et al., 2008). This weight loss was accompanied by significant alterations in lipid metabolism, as revealed by mass spectrometry-based lipidomic analysis (Fig. 1C, D). The relative abundance of lipid classes showed a diet-dependent pattern of lipid accumulation (Fig. 1C). For the most abundant lipid classes - triacylglycerides (TG), diacylglycerides (DG), and lysophosphatidylethanolamine (LPE) - both HFD and HSD conditions led to increased absolute values per body weight (Fig. 1D). Specific lipid species were enriched depending on the diet: HFD-fed females exhibited higher levels of lysophosphatidylcholines (LPC and LPCH), carnitines (CAR), ceramides (CER), and plasmalogen

phosphatidylethanolamine (PE-O). In contrast, HSD-fed females had elevated levels of cholesteryl esters (CE) (Fig. 1C, D), reflecting an obesity-like metabolic phenotype. Notably, these changes aligned with patterns seen in mammalian models of diet-induced obesity (Abshirini et al., 2021; Eisinger et al., 2014a; Eisinger et al., 2014b). Additionally, phosphatidylglycerol (PG) levels were reduced in HFD-fed females compared to both control diet (CD) and HSD groups, indicating potential lipid metabolism remodeling under fat-enriched feeding conditions.

Finally, we performed bulk RNA-sequencing (RNA-seq) analysis of whole flies to address possible transcriptional changes induced by the diets. Principal component analysis (PCA) of CD-, HFD-, and HSD-fed females showed no clear separation between dietary groups (Fig. 1E). Moreover, only a small number of differentially expressed genes (DEGs, LFC > 0, adjusted p-value< 0.1) were detected: 27 genes were downregulated in the HSD group compared to CD, while only two genes were downregulated in the HFD group (Fig. 1F). No downregulated genes were shared between HSD and HFD groups. In contrast, more genes were upregulated: 30 genes were uniquely upregulated in the HSD group and 18 genes were uniquely upregulated in the HFD group compared to the CD group, with only 4 genes overlapping between these conditions (Fig. 1F). We conducted Kyoto Encyclopedia of Genes and Genomes (KEGG) and gene ontology (GO) analyses to identify enriched pathways associated with these DEGs. However, no significant pathway enrichment containing at least three genes was found for most conditions with the exception of upregulated genes upon HFD. Here, the genes Fad2, CG18609, CG7910, eloF, CG16904, CG9459, CG9458, CG6432, and CG30008 associated with the term 'fatty acid metabolic process' (Fig. 1G, Supplemental Table 1). Furthermore, in both the HSD and HFD, the gene InR was significantly upregulated indicating a metabolic response to the dietary conditions (Supplemental Table 1).

These results confirm the successful establishment of the maternal obesity model, with both HFD and HSD inducing significant changes in body weight and lipid metabolism in females, making this model suitable for studying the effects on progeny outcomes.

## 3.2. Developmental programming by maternal diets leads to differential transcriptional responses in the offspring

To assess the impact of maternal diets on the next generation at the molecular level, we conducted transcriptomic analyses of progeny at days 0, 10, and 50. These time points were chosen to capture immediate, mid-term, and long-term transcriptional responses to maternal diet exposure. RNA-seq was performed to unbiasedly investigate gene expression changes across multiple conditions. When analyzing all timepoints from male and female flies, the PCA, which takes into account all expressed genes, indicated that samples are largely separated by sex (Fig. 2A). To remove the sex-specific gene expression effects, we analyzed females and males separately. Here, the samples clustered according to their age, indicating that the transcriptional changes accompanied with the ageing process are masking the diet-driven changes (Fig. 2B). To reveal more specific changes driven by the different maternal diets, we estimated and subsequently removed the ageing signature from all samples. Intriguingly, males then started to cluster according to the respective maternal diet, while females did not show any specific clustering behavior (Fig. 2C). Next, to investigate the transcriptional changes influenced by different ages, sexes, and diets, we analyzed the RNA-seq data by focusing on DEGs under three primary conditions: main effect of age, diet, and total effect (Fig. 2D). To this end, we first calculated the DEGs across diets on day 10 or day 50 in comparison to day 0 (Day - main effect). This analysis highlights agespecific changes, independent of diet. In both males and females, we observed an increase of DEGs upon ageing, with males dramatically altering their transcriptome on day 50 (Fig. 2E). Then, we calculated the number of DEGs with the diet as the main effect, which isolates dietinduced transcriptional changes. Here, males showed a higher number of DEGs in both diets, particularly in the HSDm group, while females

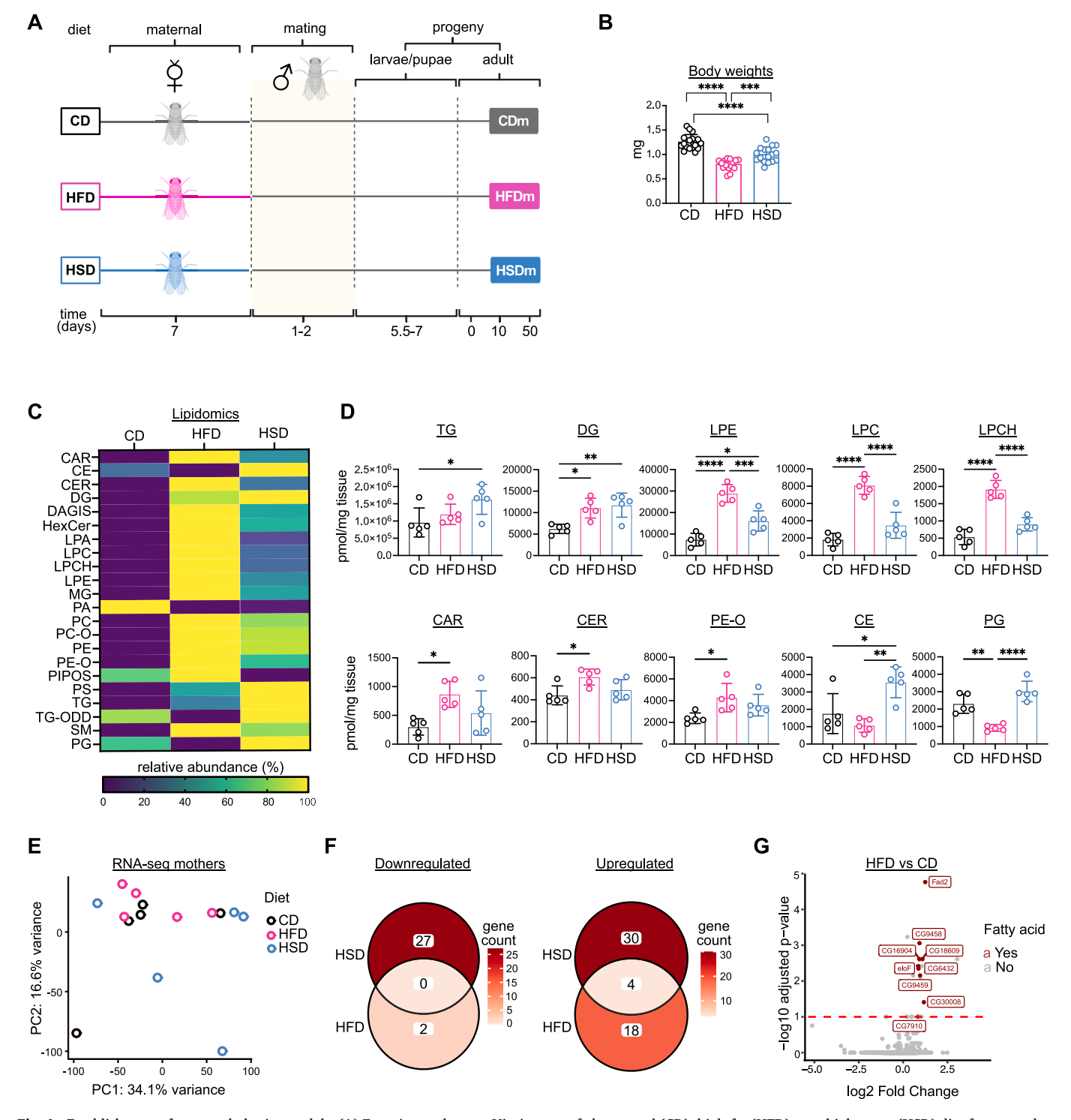


Fig. 1. Establishment of maternal obesity models. (A) Experimental setup. Virgins were fed a control (CD), high-fat (HFD), or a high-sugar (HSD) diet for seven days and subsequently mated with males on CD. Offspring from CD (CDm), HFD (HFDm), and HSD (HSDm) was kept on CD throughout life. Assays were performed on days 0, 10 and 50. Created in BioRender. Mass, E. (2025) https://BioRender.com/8nfkd2o. (B) Body weights of females after seven days of the respective diet. Circles represent single flies. Bar graphs show mean  $\pm$  SD. One-way ANOVA \* p < 0.05, \*\*\* p < 0.01, \*\*\*\* p < 0.001, \*\*\*\* p < 0.0001. (C) Heatmap illustrating the relative abundance of lipid species in female flies after seven days of exposure to respective diets. CAR: Carnitines, CE: Cholesteryl Ester, CER: Ceramide, DG: Diacylglycerol, DAGIS: Diacylglycerol Isomer, HexCer: Hexosylceramide, LPA: Lysophosphatidic Acid, LPC: Lysophosphatidylcholine: LPCH: Lysophosphatidylcholine Hydroxy, LPE: Lysophosphatidylethanolamine, MG: Monoacylglycerol, PA: Phosphatidic Acid, LPC: Phosphatidylcholine, PC-O: Plasmalogen Phosphatidylcholine, PE: Phosphatidylcholine, PE-O: Plasmalogen Phosphatidylcholine, PG: Phosphatid

showed only few DEGs overall (Fig. 2F). To capture the overall impact, DEGs were analyzed for males and females separately by considering the combined effects of diet, age and their interaction (Supplemental Tables 2, 3). This approach identifies broader transcriptional shifts, including interaction effects, while accounting for sex-specific differences. In this total effect analyses, males had thousands of up- and downregulated genes at day 50, while almost no genes were changed at day 10 when compared to day 0 (Fig. 2G). For females, the total effect was rather visible at day 10 for both diets, and decreased at day 50 (Fig. 2H). Taken together, maternal diets impact offspring transcriptomes in a sex- and age-dependent manner, with males showing pronounced age-driven transcriptional changes at day 50 and clustering by diet after removing ageing effects, while females exhibit fewer diet-specific changes and a transient transcriptional response at day 10.

Next, we analyzed unique and shared DEGs across all time points for both sexes in a diet-specific manner, comparing gene expression to the respective CDm groups. Notably, no DEGs were consistently shared across days 0, 10, and 50 for either upregulated or downregulated genes in male or female offspring (Fig. 3A). Minimal overlap was observed between two time points, with the largest overlap found in upregulated genes in HSDm males at days 0 and 50. However, GO term and KEGG pathway analysis of these overlapping genes did not reveal any meaningful enrichment. Similarly, we tested for functional enrichment of DEGs shared between day 10 and day 50 for both HSDm and HFDm female groups but found no significant terms or pathways in these analyses.

To further explore the data, we performed GO term and KEGG analyses comparing single time points across sexes and diets. The largest changes were observed at day 50 in males, with fewer terms enriched at day 0 and none at day 10 (Fig. 3B). At day 0, genes associated with the term 'cell cycle' were downregulated in both HFDm and HSDm conditions. At day 50, diet-specific differences emerged: in the HFDm condition, downregulated terms included 'axon development' and 'eye development,' while in the HSDm condition, metabolic process-related genes were specifically downregulated. A common downregulated term across both diets at day 50 was 'regulation of innate immune response.' In contrast, common upregulated terms across conditions and days included 'sperm competition' (days 0 and 50), and 'glycolysis/ gluconeogenesis,' 'microtubule bundle formation,' 'protein targeting to mitochondrion,' and 'protein targeting' (day 50). Certain processes were diet-specific: terms like 'Alzheimer's disease' and 'Parkinson's disease' were enriched in the HSDm condition, while 'pentose phosphate pathway' and 'pyruvate metabolic process' were specifically upregulated at day 50 in the HFDm condition.

In females, the largest enrichments were observed at day 10, with fewer terms identified at day 50 and none at day 0 (Fig. 3B). Similar to HFDm males at day 50, HFDm females at day 10 showed down-regulation of terms related to the Toll signaling pathway, as well as the 'sevenless signaling pathway' and 'cell cycle.' Interestingly, genes upregulated in HFDm females but downregulated in HSDm females at days 10 and 50 were associated with shared terms such as 'Alzheimer's disease,' 'Parkinson's disease,' 'oxidative phosphorylation,' and 'defense response to Gram-positive bacterium.' Conversely, genes related to terms associated with the 'cell cycle' and 'histone modification' were downregulated in the HFDm group but upregulated in the HSDm group. These findings highlight that, unlike males, females do not exhibit consistent transcriptional changes in a single direction across diets.

In summary, maternal diets lead to sex- and age-dependent transcriptional changes in offspring, with males showing pronounced age-driven responses at day 50, clustering by diet after removing ageing effects, and distinct diet-specific enrichment patterns, while females exhibit fewer diet-specific changes, transient transcriptional responses at day 10, and inconsistent trends across diets.

## 3.3. Maternal obesity induces sex-dependent physiological phenotypes in the offspring

Building on insights from our unbiased transcriptomic dataset, we investigated how maternal obesity impacts physiological traits in offspring. To this end, we performed phenotypic assays measuring body weight, glucose levels, and climbing performance at days 0, 10, and 50. These analyses aimed to uncover sex-specific physiological differences resulting from maternal HFD and HSD, offering a deeper understanding of how maternal obesity programs offspring health over time.

Indeed, males and females exhibited distinct responses to maternal diet. Male offspring from HFD- and HSD-fed mothers were lower in weight at day 0, showed a transient increase in body weight at day 10 for both maternal diets, followed by a normalization of weight by day 50 (Fig. 4A). In contrast, females displayed a delayed but sustained reduction in body weight by day 50 only in the HSDm condition (Fig. 4B), suggesting that the effects of maternal obesity on growth patterns differ by sex and evolve over time. Glucose levels, despite not significant, also followed a similar trend, with males showing higher glucose concentrations at day 0 and 10, which later normalized (Fig. 4C). Females did not show a diet- or age-specific effect on glucose levels (Fig. 4D). This early metabolic disturbance in males could reflect transient hyperglycemia induced by maternal diet exposure, while females appeared more resistant to glucose fluctuations (Fig. 4C, D).

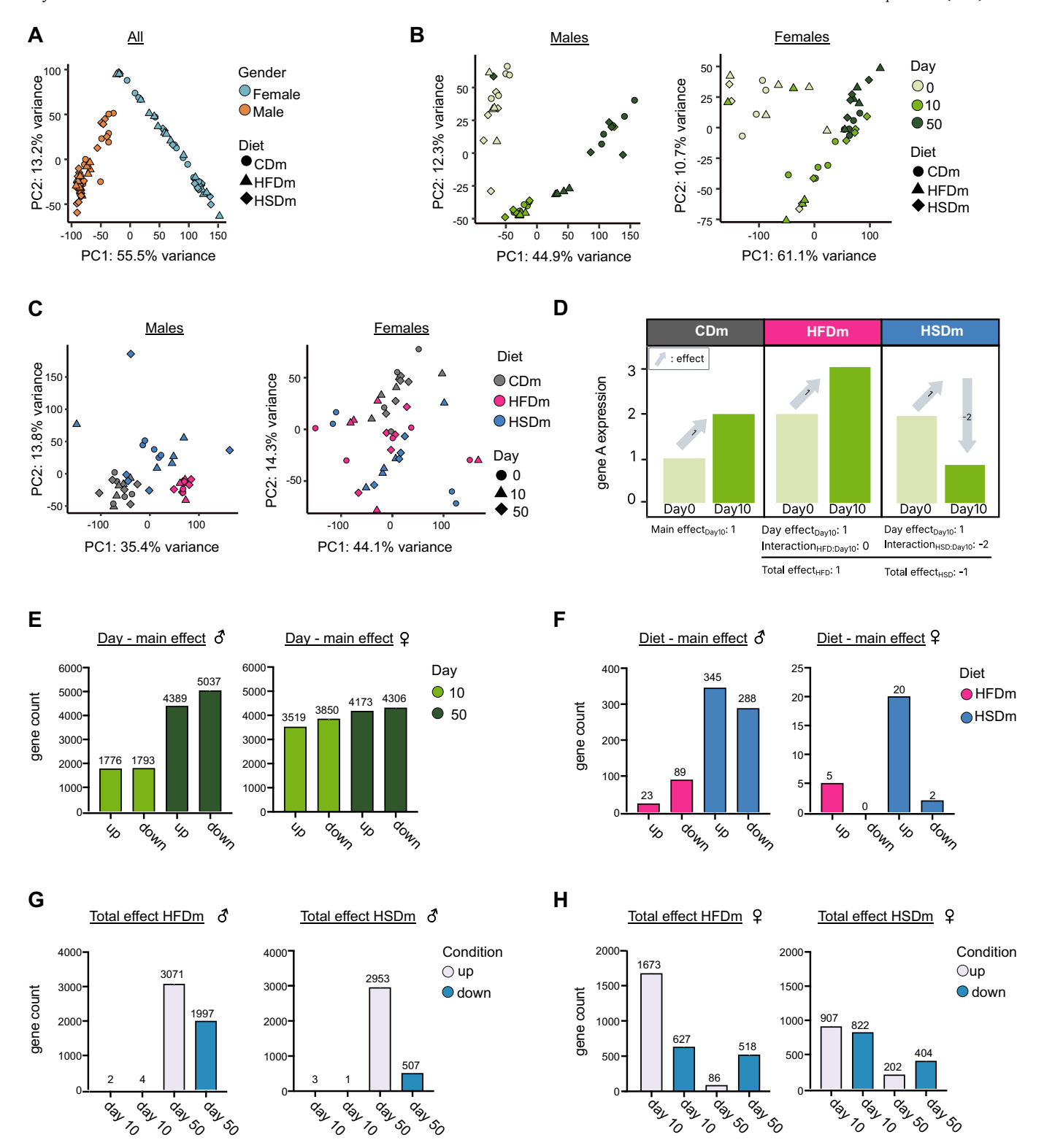
For proper locomotor output, a fine control of neuronal activity in a well-orchestrated manner is necessary. The slightest disruption in this regulation can be highly detrimental to the animal's ability to move its limbs in a coordinated fashion (Akitake et al., 2015). Thus, we performed a climbing assay as a measure of locomotor function. To this end, flies are tipped to the bottom of a vial and the height that they reach after 6 s is recorded. Male HFDm and HSDm offspring exhibited significant impairments in climbing ability by day 50 in comparison to CDm offspring, leading to almost absent motor performance due to the maternal diets (Fig. 4E). This decline was absent in female offspring, whose climbing ability remained comparable to controls across all time points, with an expected decline of climbing performance upon ageing across all dietary conditions (Fig. 4F).

Finally, we assessed the lifespan of males and females from all three maternal dietary groups. While males from the HFDm group showed a significant reduction of lifespan compared to the CDm group, HSDm did not have any effects on the overall of lifespan of the male offspring (Fig. 4G). These differences were absent in female flies (Fig. 4H), underscoring the overall resilience of females to maternal diet-induced changes.

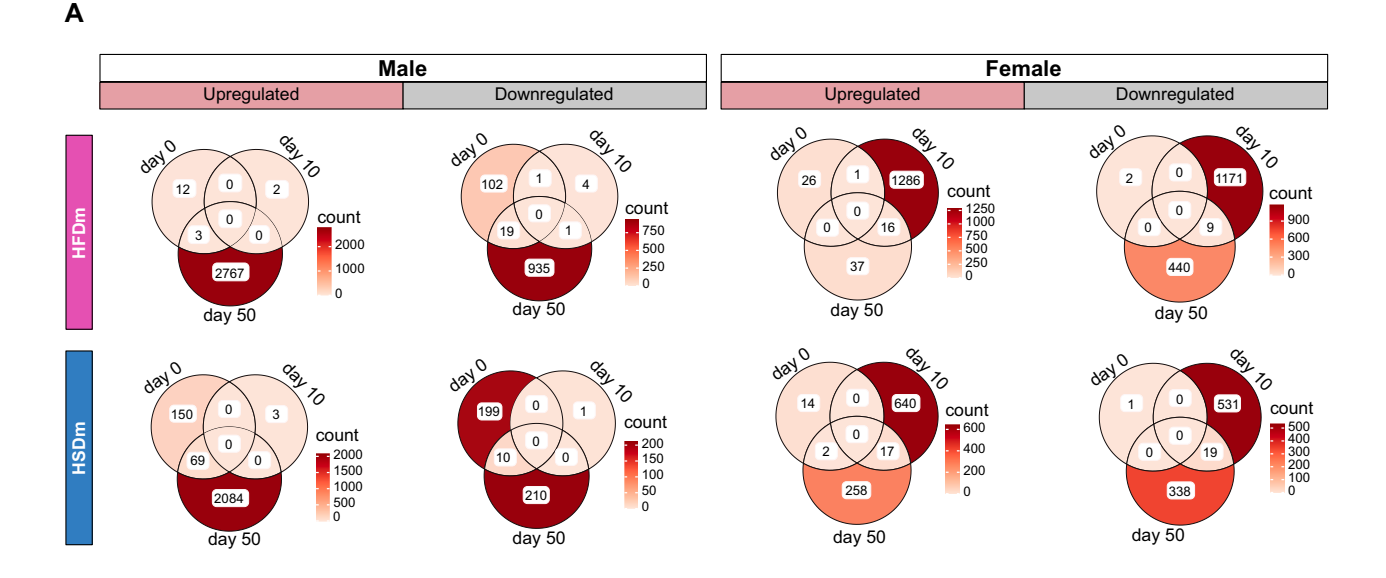
The observed sex-dependent phenotypes highlight the complex interplay between maternal diet and offspring health, with male offspring being more vulnerable to maternal diet-induced disturbances.

#### 3.4. Maternal high-fat diet leads to increased axonal degeneration

The potential neurodegenerative effects of maternal obesity were assessed by examining axonal degeneration in the offspring. We observed downregulation of genes associated with the GO terms 'axon development' and 'eye development' in males from the HFDm condition at day 50 (Fig. 3B). Similarly, in females from the HSDm group at day 10, genes associated with the GO term 'regulation of axonogenesis' and KEGG terms 'Alzheimer's Disease' and 'Parkinson's Disease' were downregulated (Fig. 3B). Given that axonal degeneration is a hallmark of neurodegenerative diseases (Richard et al., 2022a), we tested for axonal degeneration in the offspring from the different maternal diets. To assess neurodegeneration, R7 axons in the eye and their termini in the medulla layer were visualized using genetically labeled photoreceptors (GMR-Gal4 > UAS-tubulinGFP). Ten-day-old males and female offspring from all diet groups were exposed to continuous light for seven days (10,000 lx), a condition known to induce mild degeneration of axons (Richard et al., 2022a). Our results showed that male HFDm



**Fig. 2.** Maternal obesity alters offspring transcriptional profiles. (A) PCA showing transcriptional differences across analyzed samples. n = 3–5 per condition. (B) PCA of male and female progeny. (C) PCA of male and female progeny with removed day effect. (D) Pictogram depicting an example gene ("Gene A") to illustrate the difference between main effects and total effects in a factorial design. Gene expression is shown for three diet groups (CDm, HFDm, HSDm) at two timepoints (Day 0 and Day 10). Arrows represent the direction and magnitude of expression changes. The main effect of Day 10 reflects the overall time-dependent change across all diets (estimated under CDm and irrespective of Diet). In contrast, the total effect in each dietary condition (HFDm, HSDm) combines the Day 10 main effect with the respective interaction term, highlighting how experimental context modifies the observed response. Here, while HFDm shows no interaction (total effect = main effect), HSDm has a negative interaction, resulting in a negative total effect. (E) DEG counts for the main day effects, comparing males and females at days 10 and 50 to day 0 gene expression. (F) DEG counts for the main diet effects, comparing all males and females at days 0, 10 and 50 from the HFDm or HSDm to the CDm group. (G, H) DEG counts for the total day effects in male (G) and female offspring (H) comparing each diet and day separately to CDm.



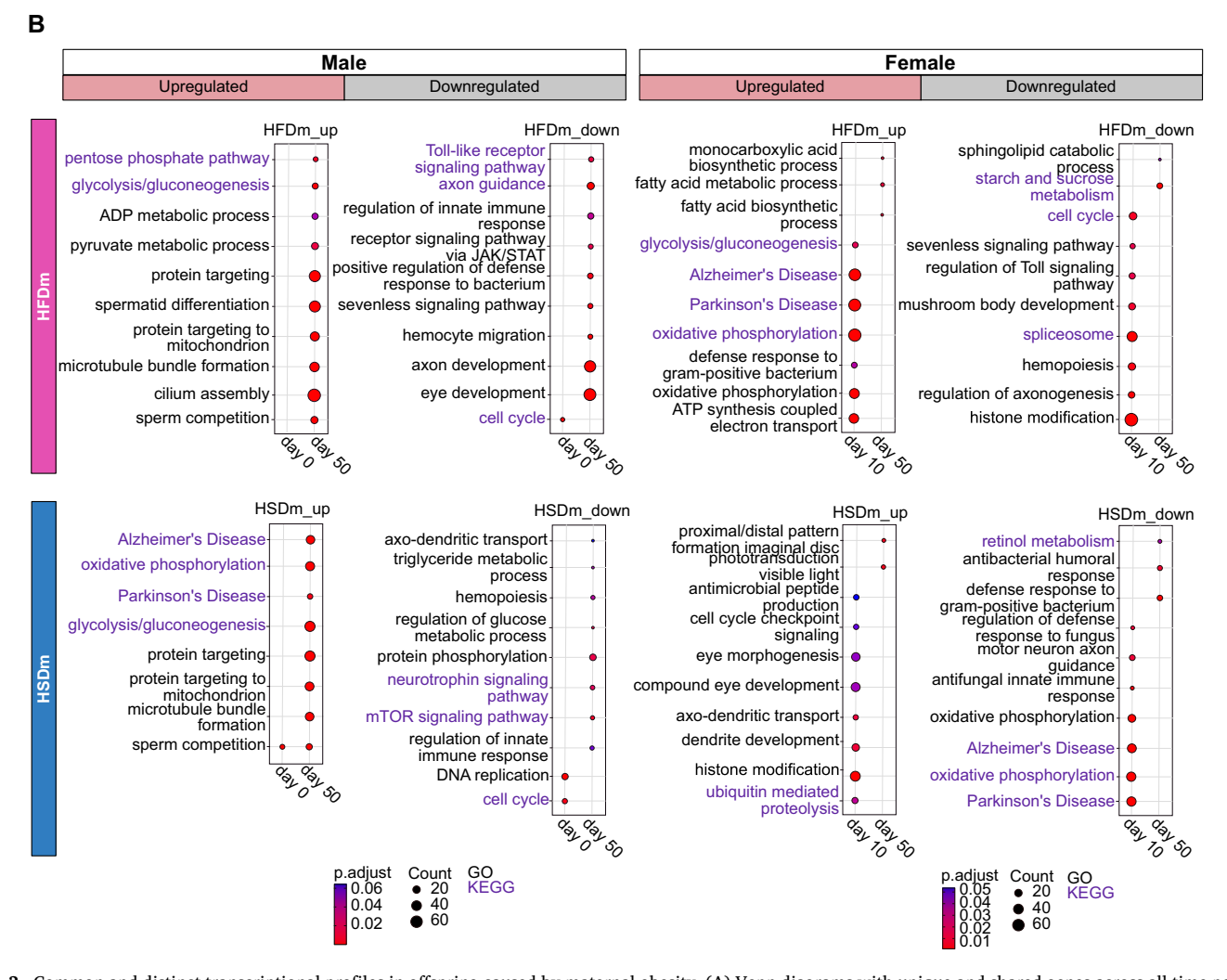


Fig. 3. Common and distinct transcriptional profiles in offspring caused by maternal obesity. (A) Venn diagrams with unique and shared genes across all time points in the respective diets compared to CDm group in male and female offspring. (B) Kyoto Encyclopedia of Genes and Genomes (KEGG) and Gene Ontology (GO) enrichment analyses of male and female offspring performed with unique genes from A.

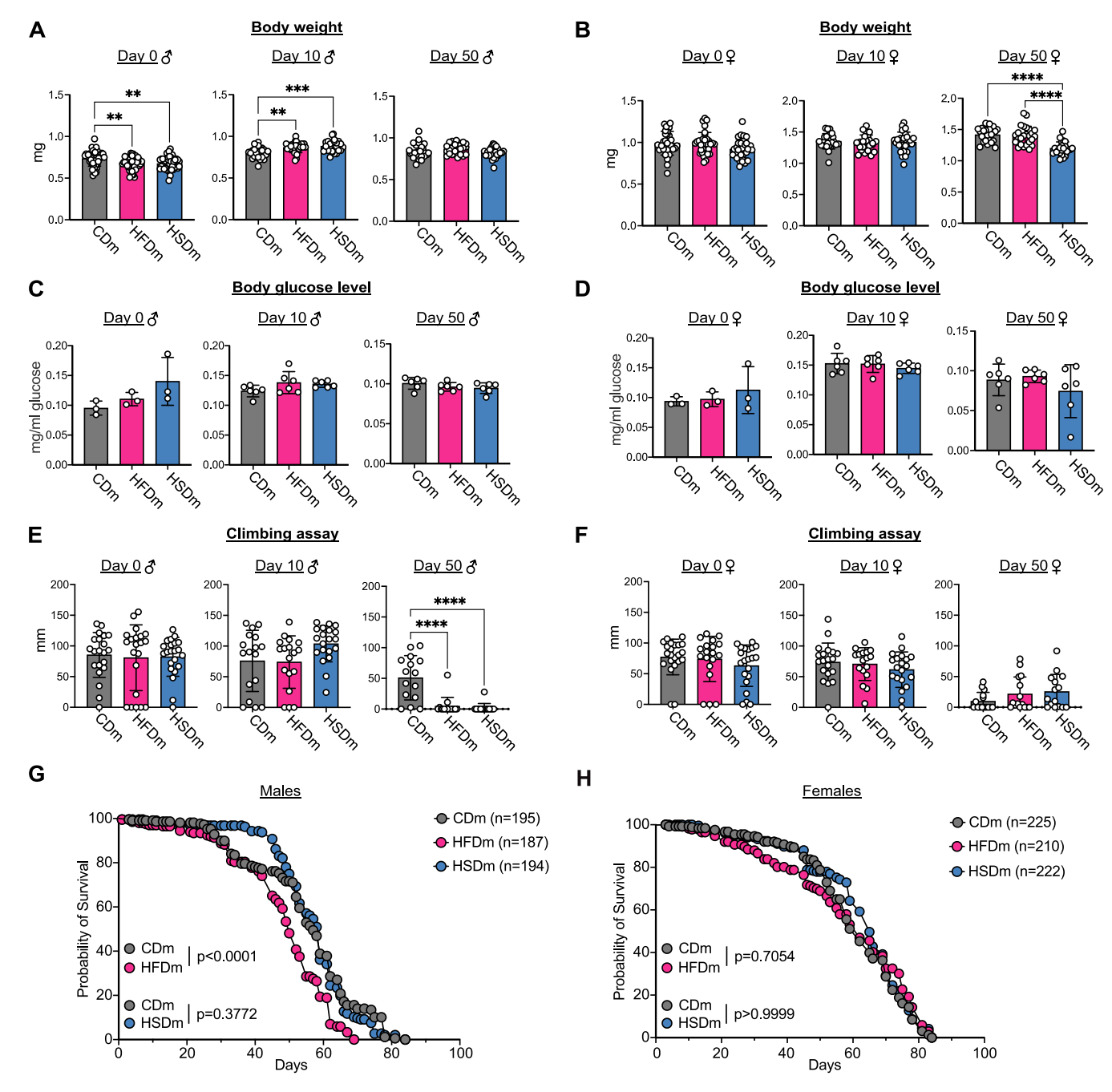


Fig. 4. Maternal diet shows sex-specific effects on organismal health in the HFDm and HSDm offspring. (A, B) Body weight of male (A) and female (B) offspring. (C, D) Circulating glucose levels of male (C) and female (D) offspring. (E, F) Climbing performance of male (E) and female (F) offspring. For A-F: Circles represent single flies. Bar graphs show mean  $\pm$  SD. One-way ANOVA \* p < 0.05, \*\* p < 0.01, \*\*\* p < 0.001, \*\*\*\* p < 0.0001. (G, H) Cumulative lifespan of male (G) and female (H) offspring. Gehan-Breslow Wilcoxon test.

offspring exhibited significant axonal degeneration, indicated by a reduced number of axonal termini in the R7 region upon light exposure compared to CDm and HSDm offspring (Fig. 5A). In contrast, female offspring did not show significant axonal degeneration across dietary conditions upon light exposure (Fig. 5B), indicating that the neurodegenerative effects of maternal obesity are both sex-specific and dietspecific. Of note, maternal diet alone did not reduce R7 axon numbers in control flies (Fig. 5A, B); in fact, female offspring showed slightly higher axon counts under standard 12 h light/12 h dark conditions (Fig. 5B). This suggests that axonal degeneration arises from the combined impact of maternal diet and light-induced stress in a sex-dependent manner.

These results underscore the long-term impact of maternal nutrition

on offspring neuronal health and highlight the greater vulnerability of male offspring to diet-induced neurodegeneration upon light-induced axonal degeneration.

#### 3.5. Maternal HFD leads to blunted immune gene expression in males

Next, we wanted to explore whether maternal diet would have an impact on immune functions in the offspring since GO terms associated to the innate immune response were identified in males and females after 10 and 50 days in both HSDm and HFDm conditions (Fig. 3B). We started by analyzing selected genes associated with the innate immune response, separating them by sex (Fig. 6A, B). In males, distinct gene clustering was observed by age, with many selected immune-relevant

Cells & Development 183 (2025) 204040

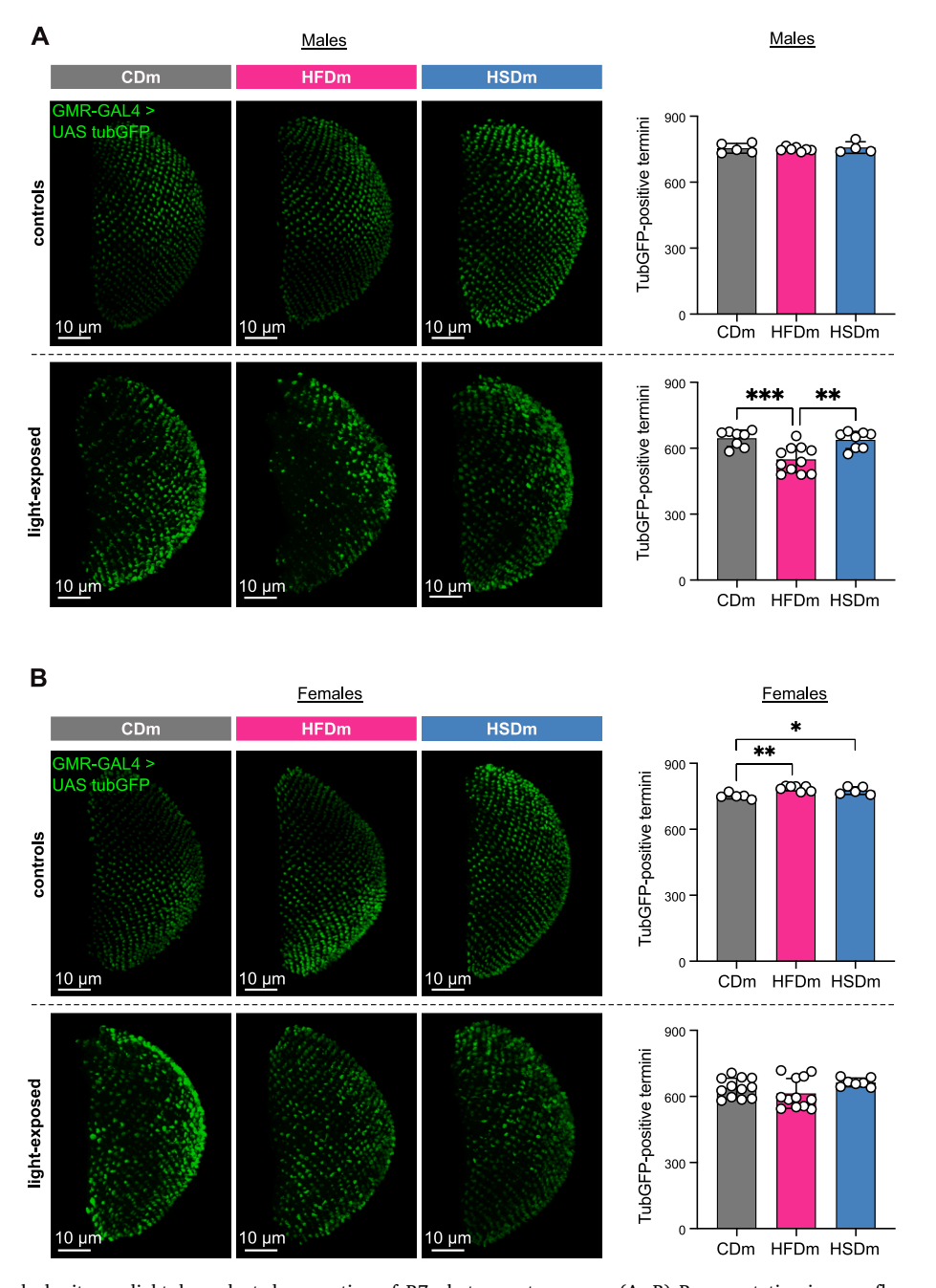


Fig. 5. Impact of maternal obesity on light-dependent degeneration of R7 photoreceptor axons. (A, B) Representative immunofluorescent pictures (left) and quantification of axonal termini (right) of male (A) and female (B) offspring that were either exposed to light (10,000 lx) over 7 days or control offspring treated with 7 days of regular 12 h light/12 h dark cycle. Scale bar: 10  $\mu$ m. Circles represent measurements for single flies. Bar graphs show mean  $\pm$  SD. One-way ANOVA \* p < 0.05, \*\* p < 0.01, \*\*\* p < 0.001, \*\*\*\* p < 0.0001.

genes being upregulated at day 50. These included anti-microbial peptides such as *Drs*, *Def*, *DptA*, *DptB*, *AttA*, *AttB*, *AttC*, *CecA1*, *CecA2* (Hanson and Lemaitre, 2020), as well as genes essential in response to pathogens, such as *Stat92E*, *drpr*, *NimB3*, *upd3*, *crq*, *Myd88*, *and Rel* (Fig. 6A). However, when comparing diets at day 50, males from the HFDm group exhibited an impaired ability to upregulate certain immune-related genes, including *Myd88*, *Rel* and *upd3* (Fig. 6C). These are primarily expressed by hemocytes, as well as other immunologically active tissues such as the fat body and the gut (L et al., 2022; Hoffmann and Reichhart, 2002). To determine whether the decreased gene expression was due to a reduction in hemocytes numbers, we quantified hemocytes at day 10 and 50 using the *Hml-GAL4* > *UAS-2xeGFP* fly line. However, we did not observe any differences in males across dietary conditions (Fig. 6D). In female offspring, an age-dependent clustering of

immune-related genes was also observed, although the differences between days 0 and 10 were minor (Fig. 6B). At day 50, females showed a similar, albeit blunted, upregulation of immune-related genes. However, in contrast to males, females did not exhibit a diet-specific clustering of immune-related genes (Fig. 6B). Notably, *upd3* expression was significantly downregulated at day 50 in both HFDm and HSDm conditions compared to CDm (Fig. 6C). Furthermore, hemocyte numbers remained unaltered (Fig. 6E).

In summary, maternal diet affects immune gene expression in the offspring: under normal conditions, males show a robust age-associated upregulation of key immune genes, but this response is significantly attenuated in HFDm males, indicating a diet-induced impairment in the normal activation of immune pathways with age; in contrast, females exhibit a blunted but diet-independent pattern of immune gene

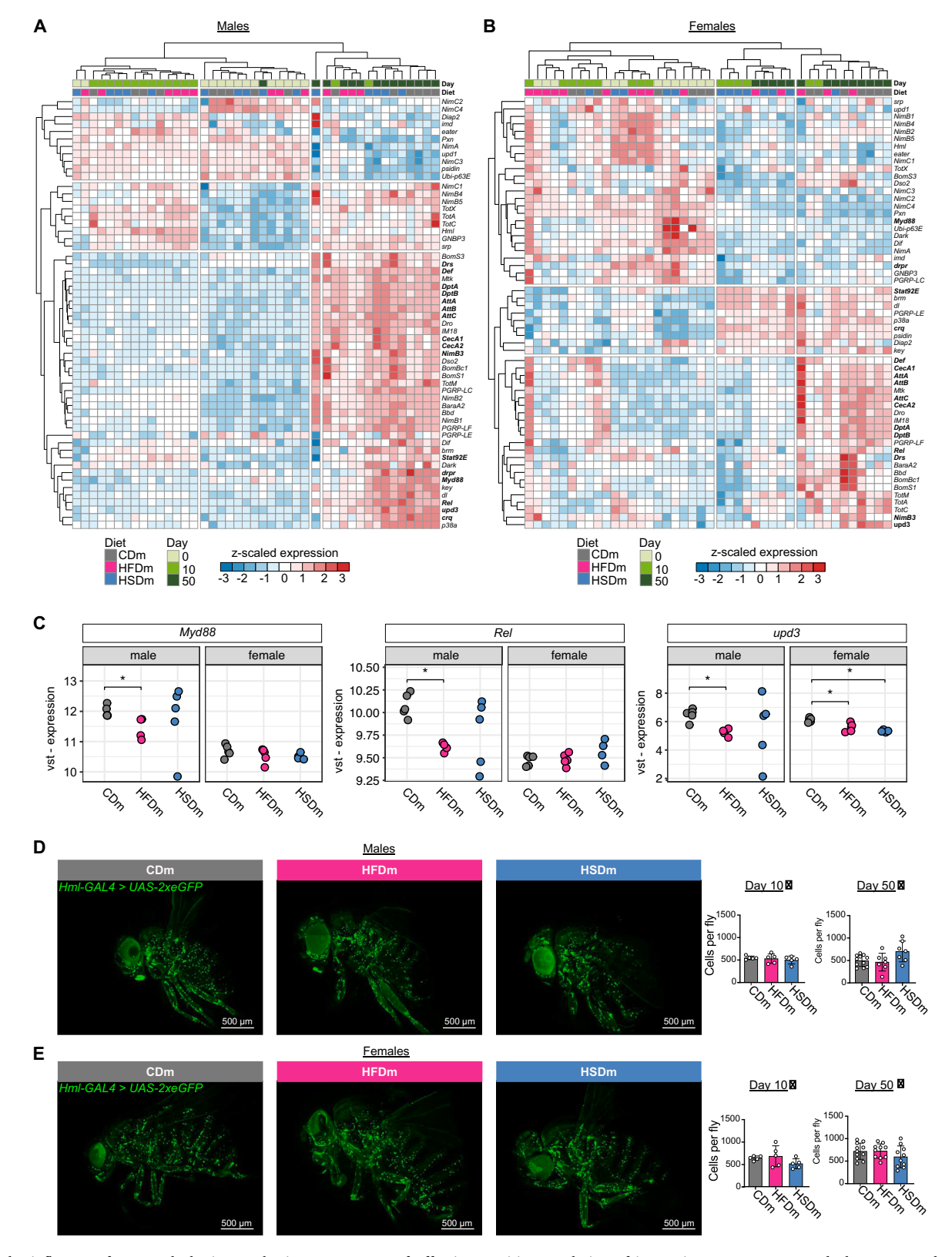


Fig. 6. The influence of maternal obesity on the immune system of offspring. Positive regulation of innate immune response and plasmatocyte density were investigated in both male and female progeny. (A, B) Heatmaps showing hierarchical expression clustering of selected genes related to the regulation immune response across all groups in male (A) and female (B) offspring. (C) Variance-stabilized gene expression counts for Myd88, Rel and upd3 at day 50 for both sexes. Wilcoxon test. \*p < 0.05, \*\*p < 0.01, \*\*\*p < 0.001. (D, E) Representative immunofluorescent pictures (left) and quantification of hemocytes (right) of male (D) and female (E) offspring. Scale bar: 500  $\mu$ m. Circles represent measurements for single flies. Bar graphs show mean  $\pm$  SD. No statistical differences could be detected using one-way ANOVA.

regulation.

#### 3.6. Developmental programming of hemocytes influence longevity

Given the link between maternal diet, immune responses, and longevity observed specifically in males in our study, we investigated whether maternal obesity impacts lifespan in a hemocyte-dependent manner. To this end, we used the  $w^{1118}$ ;  $Hml\Delta$ -Gal4, UAS-2xeGFP line, which enables specific gene expression in hemocytes. This line allows robust and selective targeting of hemocytes and thus serves as a suitable tool for cell-specific RNAi-mediated gene knockdown. Using this system, we generated CDm, HFDm, and HSDm males with hemocyte-specific knockdown of the NF-kB-like transcription factor Relish (Rel) or upd3 (ortholog of the mammalian interleukin-6). Intriguingly, targeting these pathways revealed a diet-specific response. In Hml-Gal4 > UAS-RelRNAi flies, the HFDm group exhibited reduced survival compared to the HSDm and CDm groups (Fig. 7A). In contrast, the HSDm and CDm groups showed survival patterns similar to  $w^{1118}$  flies (Fig. 7A, Fig. 4G). Knockdown of hemocyte-specific upd3 (Hml-Gal4 > UAS-upd3RNAi) resulted in similar survival curves across dietary conditions, with the HSDm group even showing increased survival (Fig. 7B). This indicates that hemocyte-derived upd3 contributes to the detrimental effects of maternal HFD on male offspring longevity. In its absence, the intergenerational impact of maternal obesity on lifespan appears attenuated.

Taken together, our data suggest that the developmental programming of hemocytes by maternal obesity could contribute to the off-spring's lifespan in a diet- and immune-pathway specific manner.

#### 4. Discussion

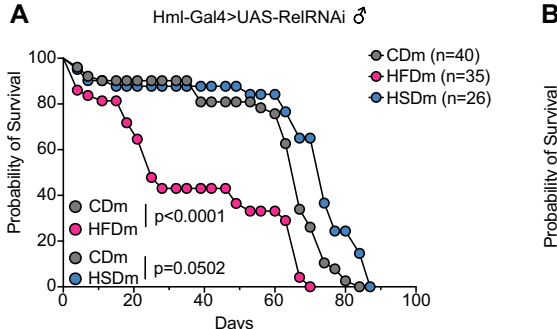
This study demonstrates the long-lasting effects of maternal obesity on offspring health and lifespan using a *Drosophila melanogaster* model, revealing critical insights into how dietary-induced maternal metabolic changes influence immune, metabolic, and neurodegenerative pathways in the next generation. Our results highlight significant sex- and age-dependent effects of maternal diet on offspring physiology, including reduced lifespan, impaired locomotor performance, and susceptibility to neurodegeneration in males. These findings align with mammalian studies showing that male offspring are often more vulnerable to maternal metabolic challenges (Viola et al., 2024; Denizli et al., 2022b; Huang et al., 2024). This sex-dependent vulnerability underscores the need to further investigate the molecular and epigenetic mechanisms that drive these differences, particularly in relation to maternal obesity.

Importantly, the age-dependent transcriptional responses observed in our study reveal a dynamic interplay between developmental programming, diet, and ageing. Males showed pronounced transcriptomic shifts at day 50, characterized by clustering according to maternal diet and widespread gene expression changes. In contrast, females displayed transient transcriptional changes at day 10 with fewer diet-specific effects, reflecting their overall resilience to maternal metabolic

disturbances. This temporal and sex-specific divergence highlights the complexity of intergenerational dietary effects, emphasizing the need for longitudinal studies to capture the full scope of these dynamics.

The neurodegenerative phenotype observed in male offspring supports the link between maternal diet and neuronal health. Downregulation of genes associated with axon development and neurodegenerative pathways, combined with significant axonal degeneration in male HFDm progeny, points to a diet-specific vulnerability of neuronal systems. These findings align with studies implicating inflammatory and metabolic dysfunctions in neurodegenerative processes, suggesting that maternal obesity primes the offspring's nervous system for early-onset degeneration (Viola et al., 2024; Denizli et al., 2022b). Interestingly, females were largely resistant to neurodegenerative outcomes, raising questions about protective mechanisms that may mitigate diet-induced neuronal stress. Although studies on maternal obesity and R7 axonal integrity in offspring are lacking, previous research has shown that HFD consumption impairs mitochondrial function in axons and leads to ocular degeneration, such as age-related macular degeneration, in rodent models (Sajic et al., 2021; Clarkson-Townsend et al., 2021; Keeling et al., 2022). Overall, our results highlight a sex-specific susceptibility to neurodegeneration induced by maternal obesity and emphasize the importance of understanding maternal diet's long-term effects on offspring neuronal health.

The immune system emerges as a central mediator of maternal diet effects, with evidence showing blunted immune responses in male offspring exposed to HFD. The reduced expression of immune genes, such as Myd88, Rel, and upd3, critical components of the JAK/STAT and Toll pathways, suggests a diminished capacity to respond to secondary challenges. Notably, these changes occur independently of hemocyte numbers, indicating that functional impairments rather than cell loss drive this immune dysregulation. This may reflect a developmental programming of hemocytes, potentially mediated by altered lipid signaling during gestation. Our study also underscores the critical role of Rel and upd3 in hemocytes, linking these pathways to offspring longevity in a diet-specific manner. Hemocyte-specific knockdowns of Rel and upd3 revealed distinct effects on lifespan: Rel is essential for the survival of HFDm offspring, while upd3 knockdown abrogates the dietinduced survival difference. However, it is important to note that Hml-Gal4 > UAS-upd3RNAi males showed an overall reduced lifespan compared to  $w^{1118}$  controls even under CD conditions, which may reflect the loss of upd3 during development or in the imago, or result from genetic background differences between the strains. Thus, while the absence of *upd3* prevents the maternal HFD-induced lifespan decline, it may also broadly impair organismal health. This highlights the contextdependent role of upd3, which may be dispensable or detrimental in some settings, yet essential for maintaining homeostasis in others. Together, these findings provide first mechanistic insights into how hemocyte-derived immune signals integrate maternal dietary cues to shape offspring longevity, offering potential targets to mitigate adverse intergenerational effects.



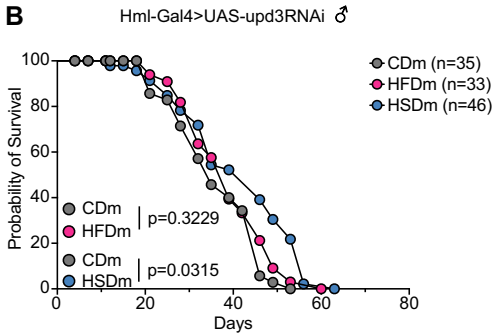


Fig. 7. Maternal obesity-induced developmental programming of hemocytes influences offspring longevity. (A, B) Cumulative lifespan of male Hml-Gal4 > UAS-RelRNAi (A) and male Hml-Gal4 > UAS-upd3RNAi (B) offspring. Gehan-Breslow Wilcoxon test.

S. Bayar et al. Cells & Development 183 (2025) 204040

Finally, the parallels between *Drosophila* and mammalian models underscore the utility of this system for studying intergenerational health impacts. The conserved nature of immune and metabolic pathways, combined with the ability to perform targeted genetic manipulations, makes *Drosophila* an invaluable tool for uncovering mechanisms underlying maternal diet effects. For example, maternal-derived lipid classes and immune mediators identified in this study could serve as therapeutic targets to ameliorate metabolic and immune dysfunctions in at-risk offspring.

In conclusion, this work highlights the multifaceted impact of maternal obesity on offspring health, including immune dysregulation, neurodegeneration, and reduced lifespan. The sex- and age-dependent nature of these effects underscores the complexity of maternal influence, while the conserved pathways identified provide a foundation for translational studies. Future research should aim to unravel the epigenetic and molecular drivers of these developmental programming mechanisms, paving the way for interventions that improve health outcomes across generations. By understanding the intergenerational effects of maternal diet, we can better address the rising global burden of obesity and its long-term consequences.

Supplementary data to this article can be found online at https://doi.org/10.1016/j.cdev.2025.204040.

#### CRediT authorship contribution statement

Seyhmus Bayar: Visualization, Methodology, Investigation, Formal analysis, Data curation, Conceptualization, Writing – original draft. Lea Seep: Methodology, Investigation, Formal analysis, Data curation. Karolína Doubková: Investigation. Jelena Zurkovic: Investigation. Margret H. Bülow: Supervision, Resources, Funding acquisition. Katrin Kierdorf: Supervision, Resources, Funding acquisition. Reinhard Bauer: Supervision, Resources, Funding acquisition. Christoph Thiele: Supervision, Resources, Funding acquisition. Gaia Tavosanis: Supervision, Methodology, Funding acquisition. Jan Hasenauer: Supervision, Resources, Funding acquisition. Elvira Mass: Formal analysis, Data curation, Conceptualization, Visualization, Supervision, Resources, Methodology, Investigation, Funding acquisition, Writing – original draft.

#### **Funding**

The work in the labs was supported by the following grants: Funded by the Deutsche Forschungsgemeinschaft (DFG, German Research Foundation) under Germany's Excellence Strategy-EXC2151-390873048 (to EM JH, CT) and CIBSS-EXC-2189, Project ID 390939984 (to KK), SFB1454 (Project ID 432325352, to EM, JH, CT), FOR5547 – Project-ID 503306912 (to EM), the Heisenberg program of the German Research Foundation (DFG) (Project ID 544402801, to KK), project grant Project ID 417982926 (to MHB), project grant Project ID 529943809 (to KK), European Research Council (ERC) under the European Union's Horizon 2020 research and innovation program (Grant Agreement No. 851257, to EM).

#### Declaration of competing interest

The authors declare no competing interests.

#### Acknowledgements

We thank Nelli Blank-Stein and Kerim Acil for support in the lab. We thank the GeneCore at EMBL for technical support and infrastructure.

#### References

Abshirini, M., Cabrera, D., Fraser, K., Siriarchavatana, P., Wolber, F.M., Miller, M.R., et al., 2021. Mass spectrometry-based metabolomic and lipidomic analysis of the

- effect of high fat/high sugar diet and Greenshelltm mussel feeding on plasma of ovariectomized rats. Metabolites 11. https://doi.org/10.3390/metabol1110754.
- Akitake, B., Ren, Q., Boiko, N., Ni, J., Sokabe, T., Stockand, J.D., et al., 2015. Coordination and fine motor control depend on Drosophila TRPγ. Nature Commun. 6 (1), 1–13. https://doi.org/10.1038/ncomms8288.
- Bray, N.L., Pimentel, H., Melsted, P., Pachter, L., 2016. Near-optimal probabilistic RNA-seq quantification. Nat. Biotechnol. 34, 525–527. https://doi.org/10.1038/
- Brookheart, R.T., Duncan, J.G., 2016. Drosophila melanogaster: an emerging model of transgenerational effects of maternal obesity. Mol. Cell. Endocrinol. 435, 20–28. https://doi.org/10.1016/j.mce.2015.12.003.
- Camilleri-Carter, T.L., Dowling, D.K., Robker, R.L., Piper, M.D.W., 2019. Transgenerational obesity and healthy aging in Drosophila. J. Gerontol.: Ser. A 74, 1582–1589. https://doi.org/10.1093/gerona/glz154.
- Catalano, P., Ehrenberg, H., 2006. Review article: the short- and long-term implications of maternal obesity on the mother and her offspring. BJOG 113, 1126–1133. https:// doi.org/10.1111/j.1471-0528.2006.00989.x.
- Ceasrine, A.M., Devlin, B.A., Bolton, J.L., Green, L.A., Jo, Y.C., Huynh, C., et al., 2022. Maternal diet disrupts the placenta-brain axis in a sex-specific manner. Nat. Metab. 4, 1732–1745. https://doi.org/10.1038/S42255-022-00693-8.
- Clarkson-Townsend, D.A., Douglass, A.J., Singh, A., Allen, R.S., Uwaifo, I.N., Pardue, M. T., 2021. Impacts of high fat diet on ocular outcomes in rodent models of visual disease. Exp. Eye Res., 204 https://doi.org/10.1016/j.exer.2021.108440.
- Cox, N., Crozet, L., Holtman, I.R., Loyher, P.-L., Lazarov, T., White, J.B., et al., 2021. Diet-regulated production of PDGFcc by macrophages controls energy storage. Science 373, eabe9383. https://doi.org/10.1126/science.abe9383.
- Denizli, M., Capitano, M.L., Kua, K.L., 2022a. Maternal obesity and the impact of associated early-life inflammation on long-term health of offspring. Front. Cell. Infect. Microbiol. 12. https://doi.org/10.3389/fcimb.2022.940937.
- Denizli, M., Capitano, M.L., Kua, K.L., 2022b. Maternal obesity and the impact of associated early-life inflammation on long-term health of offspring. Front. Cell. Infect. Microbiol. 12, 940937. https://doi.org/10.3389/FCIMB.2022.940937/ BIRTEX
- Eickelberg, V., Lüersen, K., Staats, S., Rimbach, G., 2022. Phenotyping of *Drosophila melanogaster*—a nutritional perspective. Biomolecules 12. https://doi.org/10.3390/biom12020221.
- Eisinger, K., Krautbauer, S., Hebel, T., Schmitz, G., Aslanidis, C., Liebisch, G., et al., 2014a. Lipidomic analysis of the liver from high-fat diet induced obese mice identifies changes in multiple lipid classes. Exp. Mol. Pathol. 97, 37–43. https://doi. org/10.1016/i.vexmp.2014.05.002.
- Eisinger, K., Liebisch, G., Schmitz, G., Aslanidis, C., Krautbauer, S., Buechler, C., 2014b. Lipidomic analysis of serum from high fat diet induced obese mice. Int. J. Mol. Sci. 15, 2991–3002. https://doi.org/10.3390/ijms15022991.
- Gáliková, M., Klepsatel, P., 2018. Obesity and aging in the Drosophila model. Int. J. Mol. Sci. 19, 1–24. https://doi.org/10.3390/ijms19071896.
- Ge, J., Li, C., Sun, H., Xin, Y., Zhu, S., Liu, Y., et al., 2021. Telomere dysfunction in oocytes and embryos from obese mice. Front. Cell Dev. Biol. 9. https://doi.org/ 10.3389/fcell.2021.617225.
- Hanson, M.A., Lemaitre, B., 2020. New insights on Drosophila antimicrobial peptide function in host defense and beyond. Curr. Opin. Immunol. 62, 22–30. https://doi. org/10.1016/J.COI.2019.11.008.
- Heinrichsen, E.T., Zhang, H., Robinson, J.E., Ngo, J., Diop, S., Bodmer, R., et al., 2014. Metabolic and transcriptional response to a high-fat diet in Drosophila melanogaster. Mol. Metab. 3, 42–54. https://doi.org/10.1016/j.molmet.2013.10.003.
- Hoffmann, J.A., Reichhart, J.M., 2002. Drosophila innate immunity: an evolutionary perspective. Nat. Immunol. 3 (2), 121–126. https://doi.org/10.1038/ni0202-121.
- Huang, R., Song, T., Su, H., Lai, Z., Qin, W., Tian, Y., et al., 2020. High-fat diet enhances starvation-induced hyperactivity via sensitizing hunger-sensing neurons in *Drosophila*. Elife 9. https://doi.org/10.7554/eLife.53103.
- Huang, Y., Wang, A., Zhou, W., Li, B., Zhang, L., Rudolf, A.M., et al., 2024. Maternal dietary fat during lactation shapes single nucleus transcriptomic profile of postnatal offspring hypothalamus in a sexually dimorphic manner in mice. Nature Commun. 15 (1), 1–17. https://doi.org/10.1038/s41467-024-46589-x.
- Huang, H., Balzer, N., Seep, L., Splichalova, I., Blank-Stein, N., et al., 2025. Nature. https://doi.org/10.1038/S41586-025-09190-W.
- Keeling, E., Lynn, S.A., Koh, Y.M., Scott, J.A., Kendall, A., Gatherer, M., et al., 2022. A high fat "Western-style" diet induces AMD-like features in wildtype mice. Mol. Nutr. Food Res. 66. https://doi.org/10.1002/mnfr.202100823.
- Koemel, N.A., Senior, A.M., Dissanayake, H.U., Ross, J., McMullan, R.L., Kong, Y., et al., 2022. Maternal dietary fatty acid composition and newborn epigenetic aging - a geometric framework approach. Am. J. Clin. Nutr. 115, 118–127. https://doi.org/ 10.1093/ajcn/nqab318.
- L, H., J, J., DW, M., K, S.S., D, K., G, V., et al., 2022. Fly cell atlas: a single-nucleus transcriptomic atlas of the adult fruit fly. Science 375. https://doi.org/10.1126/ SCIENCE.ABK2432.
- Lee, J.Y., Lee, J.H., Cheon, C.K., 2020. Functional characterization of gomisin N in high-fat-induced drosophila obesity models. Int. J. Mol. Sci. 21, 1–11. https://doi.org/10.3390/ijms21197209.
- Lomas-Soria, C., Rodríguez-González, G.L., Ibáñez, C.A., Reyes-Castro, L.A., Nathanielsz, P.W., Zambrano, E., 2023. Maternal obesity programs the premature aging of rat offspring liver mitochondrial electron transport chain genes in a sexdependent manner. Biology (Basel) 12, 1166. https://doi.org/10.3390/ biology/12091166
- Lourido, F., Quenti, D., Salgado-Canales, D., Tobar, N., 2021. Domeless receptor loss in fat body tissue reverts insulin resistance induced by a high-sugar diet in *Drosophila* melanogaster. Sci. Rep. 11, 1–13. https://doi.org/10.1038/s41598-021-82944-4.

- Love, M.I., Huber, W., Anders, S., 2014. Moderated estimation of fold change and dispersion for RNA-seq data with DESeq2. Genome Biol. 15, 550. https://doi.org/ 10.1186/s13059-014-0550-8.
- Martens, D.S., Plusquin, M., Gyselaers, W., De Vivo, I., Nawrot, T.S., 2016. Maternal prepregnancy body mass index and newborn telomere length. BMC Med. 14, 148. https://doi.org/10.1186/s12916-016-0689-0.
- Mase, A., Augsburger, J., Brückner, K., 2021. Macrophages and their organ locations shape each other in development and homeostasis – a *Drosophila* perspective. Front. Cell Dev. Biol. 9. https://doi.org/10.3389/FCELL.2021.630272.
- Mass, E., Gentek, R., 2021. Fetal-derived immune cells at the roots of lifelong pathophysiology. Front. Cell Dev. Biol. 9. https://doi.org/10.3389/ ECFLI 2021 648313
- Morgan, M., Obenchain, V., Hester, J., Pagès, H., 2020. SummarizedExperiment: SummarizedExperiment container. R package version 1.18.2.
- Musselman, L.P., Fink, J.L., Narzinski, K., Ramachandran, P.V., Hathiramani, S.S., Cagan, R.L., et al., 2011. A high-sugar diet produces obesity and insulin resistance in wild-type *Drosophila*. Dis. Model. Mech. 4, 842–849. https://doi.org/10.1242/ dmp.007048
- Musselman, L.P., Fink, J.L., Ramachandran, P.V., Patterson, B.W., Okunade, A.L., Maier, E., et al., 2013. Role of fat body lipogenesis in protection against the effects of caloric overload in drosophila. J. Biol. Chem. 288, 8028–8042. https://doi.org/ 10.1074/jbc.M112.371047.
- Napso, T., Lean, S.C., Lu, M., Mort, E.J., Desforges, M., Moghimi, A., et al., 2022. Diet-induced maternal obesity impacts feto-placental growth and induces sex-specific alterations in placental morphology, mitochondrial bioenergetics, dynamics, lipid metabolism and oxidative stress in mice. Acta Physiol. 234. https://doi.org/10.1111/apha.13795.
- Nayak, N., Mishra, M., 2021. High fat diet induced abnormalities in metabolism, growth, behavior, and circadian clock in *Drosophila melanogaster*. Life Sci. 281. https://doi. org/10.1016/j.lfs.2021.119758.
- Nitta, Y., Kawai, H., Maki, R., Osaka, J., Hakeda-Suzuki, S., Nagai, Y., et al., 2023. Direct evaluation of neuroaxonal degeneration with the causative genes of neurodegenerative diseases in *Drosophila* using the automated axon quantification system, MeDUsA. Hum. Mol. Genet. 32, 1524–1538. https://doi.org/10.1093/hmg/ ddac307.
- Phang, M., Ross, J., Raythatha, J.H., Dissanayake, H.U., McMullan, R.L., Kong, Y., et al., 2020. Epigenetic aging in newborns: role of maternal diet. Am. J. Clin. Nutr. 111, 555–561. https://doi.org/10.1093/ajcn/ngr326.
- Richard, M., Doubková, K., Nitta, Y., Kawai, H., Sugie, A., Tavosanis, G., 2022a. A quantitative model of sporadic axonal degeneration in the Drosophila visual system. J. Neurosci. 42, 4937–4952. https://doi.org/10.1523/JNEUROSCI.2115-21.2022.

- Richard, M., Doubková, K., Nitta, Y., Kawai, H., Sugie, A., Tavosanis, G., 2022b. A quantitative model of sporadic axonal degeneration in the *Drosophila* visual system. J. Neurosci. 42, 4937–4952. https://doi.org/10.1523/JNEUROSCI.2115-21-2022
- Ritchie, M.E., Phipson, B., Wu, D., Hu, Y., Law, C.W., Shi, W., et al., 2015. Limma powers differential expression analyses for RNA-sequencing and microarray studies. Nucleic Acids Res. 43, e47. https://doi.org/10.1093/nar/gkv007.
- Rodríguez-González, G.L., Reyes-Castro, L.A., Bautista, C.J., Beltrán, A.A., Ibáñez, C.A., Vega, C.C., et al., 2019. Maternal obesity accelerates rat offspring metabolic ageing in a sex-dependent manner. J. Physiol. 597, 5549–5563. https://doi.org/10.1113/JP278232
- Sajic, M., Rumora, A.E., Kanhai, A.A., Dentoni, G., Varatharajah, S., Casey, C., et al., 2021. High dietary fat consumption impairs axonal mitochondrial function in vivo. J. Neurosci. 41, 4321–4334. https://doi.org/10.1523/JNEUROSCI.1852-20.2021.
- Skorupa, D.A., Dervisefendic, A., Zwiener, J., Pletcher, S.D., 2008. Dietary composition specifies consumption, obesity, and lifespan in Drosophila melanogaster. Aging Cell 7, 478–490. https://doi.org/10.1111/j.1474-9726.2008.00400.x.
- Soneson, C., Love, M.I., Robinson, M.D., 2015. Differential analyses for RNA-seq: transcript-level estimates improve gene-level inferences. F1000Res 4, 1521. https://doi.org/10.12688/f1000research.7563.1.
- Sureshchandra, S., Doratt, B.M., Mendza, N., Varlamov, O., Rincon, M., Marshall, N.E., et al., 2023. Maternal obesity blunts antimicrobial responses in fetal monocytes. Elife 12. https://doi.org/10.7554/eLife.81320.
- Timpson, N.J., Wade, K.H., Smith, M.L., Goudswaard, L.J., Sattar, N., Pournaras, D.J., et al., 2024. New insights into understanding obesity: from measures to mechanisms. BMJ Med. 3, 1–11. https://doi.org/10.1136/bmjmed-2023-000787.
- Viola, M.F., Franco Taveras, E., Mass, E., 2024. Developmental programming of tissueresident macrophages. Front. Immunol. 15. https://doi.org/10.3389/ FIMMU.2024.1475369.
- Woodcock, K.J., Kierdorf, K., Pouchelon, C.A., Vivancos, V., Dionne, M.S., Geissmann, F., 2015. Macrophage-derived upd3 cytokine causes impaired glucose homeostasis and reduced lifespan in Drosophila fed a lipid-rich diet. Immunity 42, 133–144. https:// doi.org/10.1016/J.IMMUNI.2014.12.023.
- Wu, T., Hu, E., Xu, S., Chen, M., Guo, P., Dai, Z., et al., 2021. Clusterprofiler 4.0: a universal enrichment tool for interpreting omics data. Innovation (Cambridge (Mass)), 2. https://doi.org/10.1016/J.XINN.2021.100141.
- Yang, J., Tang, R., Chen, S., Chen, Y., Yuan, K., Huang, R., et al., 2023. Exposure to high-sugar diet induces transgenerational changes in sweet sensitivity and feeding behavior via H3K27me3 reprogramming. Elife 12. https://doi.org/10.7554/ELIFE.85365.
- Yu, G., Wang, L.G., Han, Y., He, Q.Y., 2012. clusterProfiler: an R package for comparing biological themes among gene clusters. OMICS 16, 284–287. https://doi.org/ 10.1089/OMI.2011.0118.